BIOCHEMISTRY
including biophysical chemistry & molecular biology

Article

pubs.acs.org/biochemistry

Role of Individual Histidines in the pH-Dependent Global Stability of Human Chloride Intracellular Channel 1

Ikechukwu Achilonu,[†] Sylvia Fanucchi,[†] Megan Cross,[†] Manuel Fernandes,[‡] and Heini W. Dirr*[,†]

[†]Protein Structure-Function Research Unit, School of Molecular and Cell Biology, University of the Witwatersrand, Johannesburg 2050, South Africa

[‡]School of Chemistry, University of the Witwatersrand, Johannesburg 2050, South Africa

Supporting Information

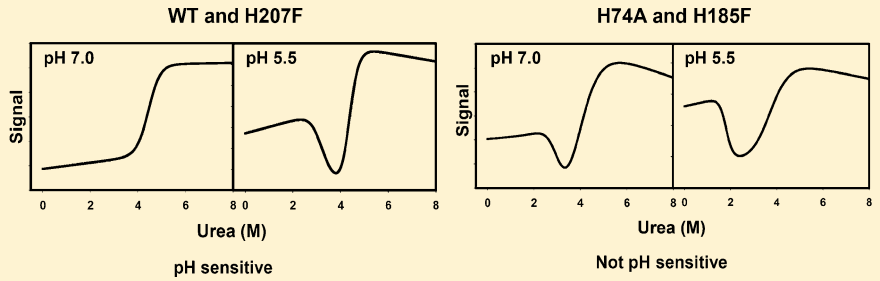

ABSTRACT: Chloride intracellular channel proteins exist in both a soluble cytosolic form and a membrane-bound form. The mechanism of conversion between the two forms is not properly understood, although one of the contributing factors is believed to be the variation in pH between the cytosol (~7.4) and the membrane (~5.5). We systematically mutated each of the three histidine residues in CLIC1 to an alanine at position 74 and a phenylalanine at positions 185 and 207. We examined the effect of the histidine-mediated pH dependence on the structure and global stability of CLIC1. None of the mutations were found to alter the global structure of the protein. However, the stability of H74A-CLIC1 and H185F-CLIC1, as calculated from the equilibrium unfolding data, is no longer dependent on pH because similar trends are observed at pH 7.0 and 5.5. The crystal structures show that the mutations result in changes in the local hydrogen bond coordination. Because the mutant total free energy change upon unfolding is not different from that of the wild type at pH 7.0, despite the presence of intermediates that are not seen in the wild type, we propose that it may be the stability of the intermediate state rather than the native state that is dependent on pH. On the basis of the lower stability of the intermediate in the H74A and H185F mutants compared to that of the wild type, we conclude that both His74 and His185 are involved in triggering the pH changes to the conformational stability of wild-type CLIC1 via their protonation, which stabilizes the intermediate state.

Chloride intracellular channels (CLICs) make up a family of ion channel proteins that are unusual in that they can exist in both a soluble form and a membrane-bound form. They are localized to the plasma membrane and membranes of most intracellular organelles where they perform an array of biological functions.[1,2] These functions include neurotransmission, ion transport, cell cycle regulation, molecular interactions, immune response, and regulation of homeostasis.[2−8] As yet, the mode of the transition of the CLICs from a soluble form to a membrane-bound form is not properly understood. Suggestions have been made that this transition could be influenced, among other things, by the difference in pH between the cytosol (~7.4) and the membrane surface (~5.5).[4,6−8] The presence of an N-terminal signal peptide that directs the protein to the membrane is still speculative for all members of the family, although studies have shown the possibility of such a peptide in CLIC4.[9] Seven classes of vertebrate CLICs have been identified to date with a high degree of amino acid sequence conservation of ~74% when they are structurally aligned.[6,10] By and large, CLICs adopt a GST-like fold with the N-domain consisting of a thioredoxin fold containing a mix of α-helices and β-sheets and the C-domain being predominantly α-helical. CLICs are therefore classified as being part of the GST superfamily.[2,6,7]

A vast number of normal and pathological processes are regulated by pH variation within the intracellular confines of the cell. Processes such as cell proliferation, cell cycle progression and differentiation, apoptosis, ligand−receptor interaction, fibrillation in Alzheimer's and Parkinsonism, and viral envelope assembly have been shown to be driven by pH variation.[11] CLICs, just like numerous eukaryotic and prokaryotic proteins, including cytokines,[12,13] prions,[14] Na^+/H^+ antiporters,[15] bacterial toxins,[16−18] viral envelope proteins,[19] and plasma proteins,[20] have been shown to alter their stability[5] and activity[21,22] in response to pH variation. Biochemically, histidine is the most likely amino acid residue that could act as a potential pH "sensor". Histidine has an imidazole side chain with a pK_a of approximately 6.5.[11] Therefore, the protonation

Received: October 5, 2011
Revised: January 10, 2012
Published: January 11, 2012

of the imidazole side chain will respond to pH variation within the physiological pH range.[11]

Several studies have shown that the side chain imidazole of histidine contributes to the global conformational changes and stability of some proteins, because of the change in entropy in its protonation state in response to pH changes within the intracellular milieu. In a transport protein such as *Escherichia coli* NhA, a single histidine residue was shown, on the basis of site-directed mutagenesis, to be responsible for a pH-induced conformational change that affects the biological activity of the protein.[15] Furthermore, histidine residues have also been implicated in the pH dependence of the stability of individual proteins.[12,13,15,16,19,23−27] Recently, Rodnin et al.[18] showed that a histidine residue in the translocation domain of diphtheria toxin is responsible for the pH-induced conformational change of the protein. In higher eukaryotes, the differentiation of function and conformational stability of histones H5 and H1 is based on a single histidine residue.[23]

There are three histidine residues within the human CLIC1 structure[7] (Figure 1A), namely, His74, His185, and His207. His74 is positioned in the N-domain of CLIC1, which contains the putative transmembrane region.[6−8,21] His185 and His207 are both on the C-domain. His185 shows a very high degree of conservation across the entire CLIC family,[6] with the exception of CLIC2, where an asparagine residue is at the same position. Lysine and tryptophan appear to be the dominant residues within the other human CLICs at the positions of His74 and His207, respectively (Figure 1B).

Given that the sensitivity of the stability of CLIC1 to pH has led to the hypothesis that low pH triggers partial unfolding of the protein,[5] we have examined the potential significance of the three histidine residues in triggering these changes. Here we study the contribution of the three individual histidine residues in CLIC1 to the observed pH-induced changes in the conformational stability of human CLIC1. We propose that, via replacement of each histidine residue in the protein with either a phenylalanine or an alanine that has nonionizable side chains, the ability of the protein to sense pH changes via these residues will be removed. Therefore, the mutant proteins are expected to exhibit unfolding behavior similar to that of the wild type at pH 7.0 and 5.5. Here, we present the global conformational stability effects of systematic single-site mutation of His74, His185, and His207 in human CLIC1 and their response to pH. We also correlate results from X-ray crystallographic studies with the spectroscopic data obtained for each mutant, and we study the global structural effect of each mutation at atomic resolution.

MATERIALS AND METHODS

Site-Directed Mutagenesis, Protein Expression, and Purification. The ORF of human CLIC1 was extracted from GenBank (entry AF034607.1), and the following mutagenic primers were designed from the ORF: 5′-ctgtatggcactgaagtg**gc**-cacagacaccaacaagattg-3′ (for H74A-CLIC1), 5′-caacctgttgc-caaagtta**ttc**atagtacaggtggtgtg-3′ (for H185F-CLIC1), and 5′-gaggccttccggggagtg**ttt**cggtacttgagcaatgcc-3′ (for H207F-CLIC1). The mutant codons are shown in bold. The primers and their corresponding reverse complements were synthesized at Inqaba Biotec (Pretoria, South Africa). Site-directed mutagenesis reactions were performed on pGEX-4T-1 encoding the wild-type *CLIC1* ORF template (a gift from S. N. Breit, Centre for Immunology, St. Vincent's Hospital and University of New South Wales, Sydney, Australia) using the QuickChange site-directed mutagenesis kit (Stratagene, La Jolla, CA) according to the manufacturer's instructions. The plasmids were sequenced at Inqaba Biotec to confirm the presence of the mutation. Plasmids encoding the appropriate mutation were used to transform *Escherichia coli* BL21(DE3) pLysS strains for overexpression of the recombinant mutant and wild-type CLIC1 (in 2× YT medium, induction with 1 mM IPTG at 20 °C for 6 h with shaking at ∼200 rpm). Cells were harvested, and the recombinant mutant CLIC1 proteins were purified as previously described.[5] Size exclusion chromatography (Sephadex G-75, 50 cm × 3.2 cm) was used to further purify the recombinant proteins. Protein purity was determined by sodium dodecyl sulfate−polyacrylamide gel electrophoresis on a 12.5% acrylamide gel slab according to the method of Laemmli.[28]

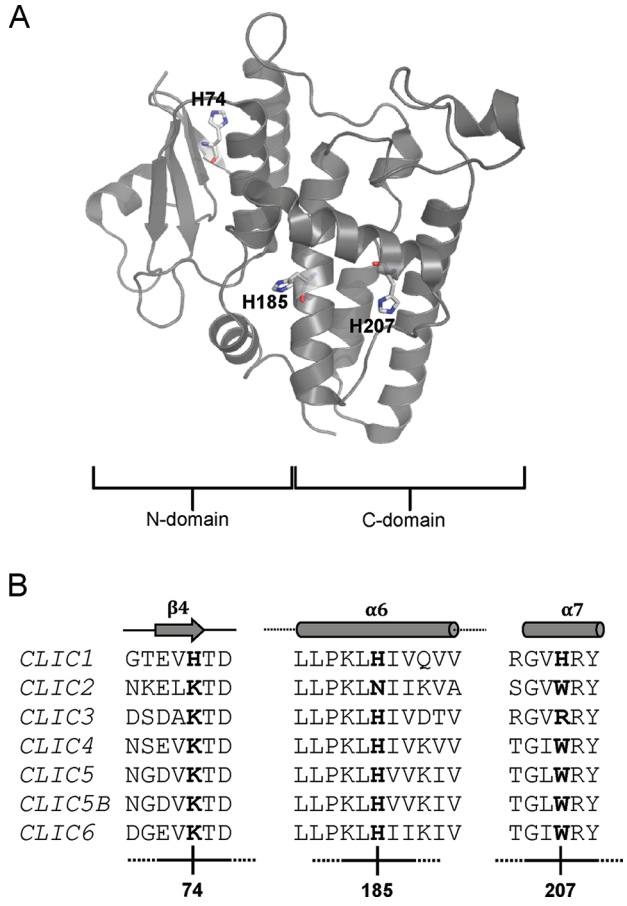

Figure 1. Structural and sequence information of human CLIC1. (A) Ribbon representation of wild-type human CLIC1 (PDB entry 1K0M) showing the N- and C-domain structures and the positions of the three histidine residues. The figure was produced with PyMol.[41] (B) Structural alignment of the seven members of the human CLIC family (cylinders represent helices, the arrow represents sheets, the solid line represents random coils, and broken lines represent truncated secondary structure). Residues in a corresponding position to the CLIC1 histidine residues are shown in bold. CLIC sequences were retrieved from the UniProtKB database (http://www.uniprot.org), and the alignment was performed with the 3DCoffee[10] web-interface program. The database accession number for the sequences used for the alignment are O00299 (CLIC1), O15247 (CLIC2), O95833 (CLIC3), Q9Y696 (CLIC4), Q9Y696 (CLIC5), Q9NZA1 (CLIC5B), and Q96NY7 (CLIC6). The numbering is based on CLIC1.

Stability Studies. Far-UV CD was used to monitor the effect of each mutation on the secondary structure of CLIC1 [2

dx.doi.org/10.1021/bi201541w | *Biochemistry* 2012, 51, 995−1004

μM in 5 mM Na_2HPO_4, 1 mM DTT, and 0.02% (w/v) NaN_3] at varying pH values (5.0−8.5). Spectra were recorded in triplicate on a Jasco model 810 CD spectropolarimeter at 20 °C. Averaged CD signals, corrected for solvent, were converted to mean residue ellipticity [Θ] (degrees square centimeters per decimole), using

$$[\Theta] = \frac{100\theta}{Cnl}$$

where C is the protein concentration (millimolar), n is the number of residues, l is the path length (centimeters), and θ is the measured ellipticity (millidegrees).

For urea-induced equilibrium unfolding, 2 μM protein [in 5 mM Na_2HPO_4, 1 mM DTT, and 0.02% (w/v) NaN_3] at pH 5.5 or 7.0 was left to equilibrate overnight in 0−8 M urea at 20 °C. The global structure was monitored by far-UV CD between 190 and 250 nm. Changes within the local environment were monitored using fluorescence by excitation of the single tryptophan residue (Trp35) located at the domain interface and eight tyrosine residues at 280 nm, and by ANS binding using an excitation wavelength of 350 nm and an emission wavelength of 460 nm (using a Perkin-Elmer LS50B luminescence spectrometer) as previously described.[5] The reversibility of CLIC1 denaturation under these conditions has been previously confirmed.[5] Four different probes were used to monitor the global unfolding: (i) ellipticity at 222 nm to monitor the secondary structure, (ii) fluorescence at 345 nm, which is the peak fluorescence intensity of the native protein and measures the tertiary structural environment about Trp35, (iii) fluorescence at 310 nm, and (iv) intensity-averaged emission wavelength (IAEW), which was used to monitor the presence of the intermediate due to wavelength shifts. IAEW was calculated using the equation

$$\text{IEAW} = \left(\sum \lambda_i \times F_i\right) / \sum F_i$$

where λ_i is the wavelength and F_i is the fluorescence intensity at λ_i. The data from equilibrium unfolding experiments were globally fit to either a two-state monomer (N ↔ U) model or a three-state monomer (N ↔ I ↔ U) model using Savuka version 6.2.26.[29,30] The thermodynamic parameters, ΔG_{H_2O} (kilocalories per mole) and m values (kilocalories per mole per molar), obtained from the global fits (using the linear extrapolation method) were used to calculate the fractional population of each species from the equilibrium constants.[31]

Protein Crystallization, X-ray Diffraction, and Structure Solution. The optimal conditions for crystallization of the three histidine mutant CLIC1 proteins were predetermined using the Hampton Index HR2-144 solutions for crystal growth at pH 5.5, 6.5, and 7.0 (Hampton Research). Briefly, crystals of recombinant H74A, H185F, and H207F human CLIC1 mutants were grown by the hanging drop vapor diffusion method at 293 K using a 24-well greased VDX plate (Hampton Research). H185F-CLIC1 and H207F-CLIC1 were grown in reservoir buffer comprising 0.1 M Bis-Tris (pH 6.5), 0.02 M $CaCl_2 \cdot 2H_2O$, and 30% (v/v) PEG 550 monomethyl ether (0.5−1.0 mL/well). H74A-CLIC1 was grown in reservoir solution containing 0.1 M Tris-HCl (pH 6.5), 0.15 M KBr and 30% (w/v) PEG 2000 monomethyl ether (0.5 mL/well). Each hanging drop (2, 6, and 8 μL) was made by mixing an equal volume of a stock protein solution [10 mg/mL in 0.1 M Tris-HCl (pH 6.5), 5 mM DTT, and 0.02% (w/v) NaN_3] with the reservoir solution. The crystals were harvested, soaked in a cryoprotectant [25% (v/v) glycerol in the mother liquor], mounted on a cryoloop, and snap-frozen in liquid nitrogen. X-ray diffraction data were collected on a Bruker X8 PROTEUM X-ray diffractometer equipped with a Microstar copper rotating anode generator, Montel Optics, a PLATINUM 135 CCD detector, and an Oxford CryoStream Plus system. Crystals were cooled to 113 K in a stream of nitrogen during data collection, and images covering an oscillation angle of 0.5° per frame were collected. The data sets were indexed with APEX and SAINT. The structures were determined by molecular replacement using PHASER[32,33] implemented in the CCP4i suite of programs.[34] The molecular replacement search model structure for H74A-CLIC1 and H207F-CLIC1 was PDB entry 3O3T, while the search model structure for H185F-CLIC was PDB entry 1K0M.[7] Search models were chosen on the basis of the space group of the crystal. The structure of H74A-CLIC1 was optimized with a development version of PDB-REDO.[35] The models were refined with REFMAC,[36] and model building was performed with COOT.[37] Solvent molecules were added to the models after several rounds of refinement. Stereochemical validation of the models was performed using PROCHECK[38] and MOLPROBITY.[39] The data collection and refinement statistics are listed in Table 1. SPDBV version 4.0[40] was used to align two or more structures and compute H-bonding. PyMol[41] was used to generate images of the structures.

RESULTS

Effect of a Single Histidine Mutation on the Secondary Structure of CLIC1. In this study, the three histidine residues of human CLIC1 were mutated to either alanine or phenylalanine to understand the roles the individual histidine residues play in pH-induced conformational stability changes in the protein. The decision about whether the histidine should be mutated to a phenylalanine or an alanine was based on the crystal structure of wild-type CLIC1 (PDB entry 1K0M). Alanine was preferred at position 74 because the His74 side chain is exposed on the surface of 1K0M. Therefore, introducing phenylalanine, with its large hydrophobic side chain, at that position may cause unwanted structural alterations within that region. Alanine is the better choice in this instance because it has a smaller, less hydrophobic side chain that is more suitable to the surface of a protein than phenylalanine. At positions 185 and 207, however, phenylalanine is preferred because the His185 and His207 side chains are more buried within 1K0M. Therefore, to prevent the creation of a cavity within these regions, phenylalanine is the better choice for replacement of His185 and His207.

The effect of each mutation on the secondary structure was monitored by far-UV CD from 190 to 250 nm, at pH values ranging from 5.0 to 8.5. This was compared to the wild type, which has been previously studied.[5] The far-UV CD trace of each mutant overlays with the wild-type trace (results not shown), indicating that the mutation does not induce conformational changes to the native state and CLIC1 maintains predominantly helical secondary structure from pH 5.5 to 8.5. Therefore, we concluded that the mutation did not result in the gross modification of the native structure of the mutant proteins.

Effect of a Single Histidine Mutation on the Conformational Stability of CLIC1. To assess the individual effect of the three histidine residues on the pH-induced changes in the conformational stability of CLIC1, urea-induced equilibrium unfolding studies were performed on the mutant

Table 1. Crystallographic X-ray Data Collection and Refinement Statistics for Human CLIC1 Mutants H74A, H185F, and H207F

	H74A	H185F	H207F
buffer/salt	0.1 M Tris-HCl/ 0.15 M KBr (pH 6.5)	0.1 M Bis-Tris/ 0.05 M $CaCl_2$ (pH 6.5)	0.1 M Bis-Tris/ 0.05 M $CaCl_2$ (pH 6.5)
PEG (% w/v)	2000 (30%)	550 MME (30%)	550 MME (30%)
PDB entry	3SWL	3QR6	3P90
	Data Collection via CCD		
wavelength (Å)	1.5418	1.5418	1.5418
space group	$P2_12_12_1$	$P2_1$	$P2_12_12_1$
unit cell dimensions	a = 82.2 Å	a = 35.3 Å	a = 42.4 Å
	b = 41.5 Å	b = 82.1 Å	b = 65.5 Å
	c = 66.7 Å	c = 41.6 Å	c = 83.3 Å
	$\alpha = \beta = \gamma = 90°$	$\beta = 95.8°$	$\alpha = \beta = \gamma = 90°$
asymmetric unit content	1	1	1
resolution range (Å)	51.8−2.4	41.0−1.8	51.5−2.3
no. of observations	223713	212861	283158
no. of unique observations	48426	22460	10799
completeness (%)	98.8 (74.9)	98.1 (87.9)	99.6 (97.2)
R_{sym} (%)	19.7 (84.1)	17.8 (63.9)	29.7 (77.4)
$I/\sigma(I)$	10.9 (1.37)	12.1 (2.51)	15.1 (2.65)
	Refinement		
resolution (Å)	51.8−2.4	41−1.8	51.5−2.3
R_{cryst}, R_{free}	0.242, 0.338	0.202, 0.257	0.207, 0.304
no. of reflections (working/test)	9965/682	22383/1249	10799/733
no. of protein atoms	1818	1855	1855
no. of solvent molecules	93	199	119
rmsd[a] for bond lengths (Å)	0.016	0.024	0.017
rmsd[a] for angles (deg)	1.57	1.97	1.57
rmsd[a] for ΔB of bonded atoms (mm/ss)[b]	0.78/2.09	1.30/3.44	0.28/1.59
$\langle B \rangle$ for protein (Å^2)	35.5	22.3	16.6
Ramachandran plot (%)			
most favored	99.1	99.5	100
generously allowed	0.9	0.5	0
disallowed	0	0	0

[a]Root-mean-square deviation. [b]mm, main chain−main chain; ss, side chain−side chain.

proteins, and the results were compared to those of the wild type at pH 7.0 and 5.5. The fluorescence at 310 nm and IAEW unfolding traces of H74A and H185F at pH 7.0 display a biphasic transition between the folded (N) and unfolded (U) states as shown in Figure 2. This indicates the presence of a stable intermediate state (I) along the unfolding transition of H74A and H185F mutants at pH 7.0. This intermediate was not detected for H207F-CLIC1 or the wild type, where the unfolding trace produces a single sigmoidal (monophasic) transition at pH 7.0 when monitored both with ellipticity at 222 nm and with tryptophan fluorescence. At pH 5.5, all three mutants and the wild type display a biphasic unfolding transition. The presence or absence of a stable intermediate state along the unfolding transition of the mutants and wild type was confirmed by binding of ANS to exposed hydrophobic patches in the intermediate state (Figure S1 of the Supporting Information). ANS did not bind to the native or denatured states of any of the mutants or the wild type. ANS binding (as detected by a blue shift in the emission wavelength to 460 nm and an increase in fluorescence intensity) was identified under mild denaturing conditions for H74A-CLIC1 and H185F-CLIC1 at pH 7.0 and for all the mutants as well as the wild type at pH 5.5. The presence of the intermediate state was further confirmed by a plot of the fractional population of the intermediate versus the urea concentration as calculated from the thermodynamic data (Figure 3). The data show that the intermediate is highly populated at pH 7.0 and 5.5 in the case of H74A-CLIC1 and H185F-CLIC1, but it is only significantly populated at pH 5.5 for the wild type and H207F-CLIC1.

The ΔG (kilocalories per mole) and the m value (kilocalories per mole per molar) were calculated from the global fit to urea-induced equilibrium unfolding. Figure 4 shows the ΔG values of the three mutants and the wild type at pH 7.0 and 5.5 for the unfolding transitions (N → U, N → I, and I → U). The data show that the unfolding profile of the H74A and H185F mutants differs from that of the wild type, while the unfolding profile of H207F is similar to that of the wild type. Furthermore, ΔG_{NI} and ΔG_{IU} of H74A and H185F do not significantly change with pH. The ΔG_{NU} values of all three mutants at pH 5.5 are lower than that of the wild type, indicating a general destabilization at this pH. The m value is indicative of the degree of denaturant-sensitive surface area exposed during an unfolding transition (Table 2). It is defined by the gradient of the unfolding curve, which is also a measure of the cooperativity of unfolding. The m values for the CLIC1 histidine mutants followed a trend similar to that of the ΔG values, indicating that the unfolding cooperativity of H74A and H185F is no longer sensitive to pH whereas that of H207F and the wild type is.

Effect of a Single Histidine Mutation on the Local Structural Environment. In this study, the crystal structures of the H74A (PDB entry 3SWL), H185F (PDB entry 3QR6), and H207F (PDB entry 3P90) mutants of human CLIC1 were determined at resolutions of 2.35, 1.78, and 2.30 Å, respectively. Table 1 shows the statistics derived from the X-ray diffraction and structure refinement data analysis. The electron densities of the final models are properly defined for residues 6−241 for all three mutants. Residues 238−241 were excluded because of poor electron density in the final model of H74A. The electron density at the point of mutation is consistent for alanine at position 74 in H74A and phenylalanine at positions 185 and 207 in H185F and H207F, respectively. The C^α rmsd values between the wild-type structure and the structures of the three mutants (0.57 Å, 215 atoms for H74A; 0.76 Å, 218 atoms for H185F; 0.51 Å, 219 atoms for H207F) indicate that the replacement of histidine with either alanine or phenylalanine did not severely alter the backbone structure of the mutants.

His74 is located on β4 in the N-domain and makes a stable H-bond with side chains on α3 and β3 in the N-domain. His74 makes a hydrogen bond with two water molecules (w-497 and w-564). w-497 forms an H-bond with Glu72, thus mediating the interaction between His74 and Glu72 (also termed an alternating ionic bridge interaction or electron sharing network),[42−44] while w-564 appears to stabilize the local environment via an indirect H-bond interaction with Thr75

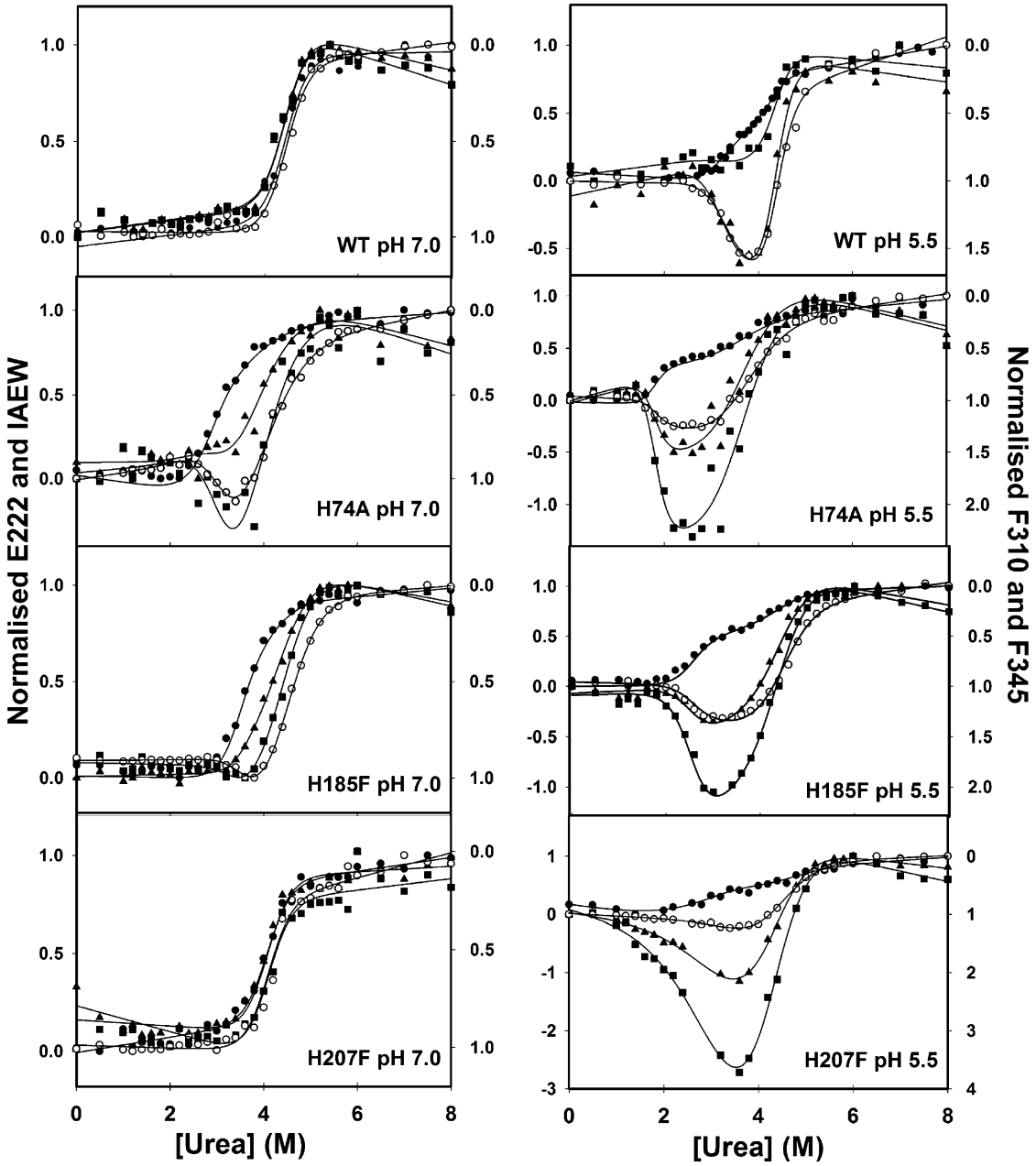

Figure 2. Urea-induced equilibrium unfolding trace curves for the wild type and each of the mutants. The urea-induced equilibrium titration experiments were conducted at 20 °C and pH 7.0 (left) and pH 5.5 (right). The unfolding was monitored by ellipticity (E_{222}) at 222 nm (●), fluorescence intensity (F_{310}) at 310 nm (■) and (F_{345}) 345 nm (▲), and IAEW (○). Each point is an average of three replicates. Data were globally fit using Savuka[29,30] version 6.2.26 and normalized, such that 0 and 1 on the *y*-axes correspond to the folded and unfolded states, respectively.

(Figure 5A). The replacement of His74 with alanine results in the loss of these H-bond interactions with both water molecules (Figure 5D), thus making the environment more hydrophobic. Loss of *w*-497 results in the displacement of the Glu72 side chain by approximately 3.2 Å compared to the wild-type Glu72 residue (using the C^{δ} atom as a reference atom). An H-bond is then formed between Glu72 and a water molecule more than 7 Å from the point of mutation.

His185, located on helix α6 of the C-domain, interacts directly or indirectly via water molecules with residues on three secondary structures (helices α7−α9). Four water molecules are involved in this process (Figure 5B), with two of the water molecules (*w*-359 and *w*-254) making direct H-bonds with the imidazole ring of His185. The carbonyl oxygen atom of His185 forms an H-bond with Gln188 and Val189. Asp226 forms an alternating ionic bridge interaction with His185 via *w*-359 and *w*-254, thereby stabilizing the local environment. The replacement of His185 with phenylalanine results in a loss of H-bonding with those two water molecules (*w*-359 and *w*-254) (Figure 5E). There is no H-bonding interaction with the phenylalanine side chain; thus, the H-bonding network is severely altered by the introduction of phenylalanine at position 185.

Because the imidazole side chains of both His74 and His185 form interactions only with water molecules, the effect of protonation of the imidazole in the native state will not be as pronounced as if the H-bond interactions were formed with side chains. However, the network of interactions between the

dx.doi.org/10.1021/bi201541w | *Biochemistry* 2012, 51, 995−1004

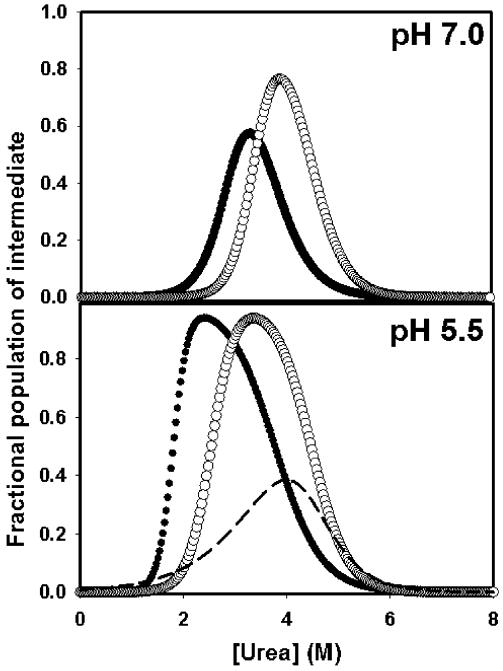

Figure 3. Fractional populations of the intermediate state of mutant CLIC1. The populations were calculated using the thermodynamic parameters obtained from global fitting of unfolding data for each mutant CLIC1 at pH 7.0 and 5.5: H74A (●), H185F (○), and H207F (– – –).

waters and the residues with which they interact is likely to be affected by protonation of the imidazole. Furthermore, this effect may be different depending on the state that the protein assumes (i.e., native, intermediate, or denatured) as described in Discussion.

No H-bond contact is made between the imidazole side chain of His207 and any of the water molecules or amino acids within its vicinity. However, one of the water molecules does form an H-bond interaction with the backbone carbonyl oxygen atom of His207 (Figure 5C). Introduction of phenylalanine at position 207 alters this H-bonding network. The water molecules that were involved in H-bonding within the local environment appear to be displaced because of the increased hydrophobicity within the environment. No H-bond contact is made with the phenylalanine side chain; therefore, no extra stability is evident (Figure 5F).

Table 2. *m* Values (kcal mol^{-1} M^{-1}) of Wild-Type and Mutant CLIC1 Determined from Globally Fit Far-UV CD and Tryptophan Fluorescence Curves

	equilibrium transition 1		equilibrium transition 2	
protein	pH 7.0	pH 5.5	pH 7.0	pH 5.5
wild type	2.4 ± 0.8	2.4 ± 0.5		3.0 ± 0.3
H74A	2.0 ± 0.5	4.0 ± 1.3	1.4 ± 0.1	1.3 ± 0.2
H185F	2.5 ± 0.4	2.6 ± 0.3	1.7 ± 0.1	1.7 ± 0.7
H207F	2.3 ± 0.2	0.7 ± 0.3		1.2 ± 0.2

DISCUSSION

Previous studies have shown that although the secondary and tertiary structures of native wild-type human CLIC1 are not affected by pH, the stability of the protein is pH-dependent. CLIC1 unfolds via a two-state transition at pH 7.0 and a three-state transition at pH 5.5 where a stable intermediate can be detected at equilibrium under mild denaturing conditions.[5] Similar observations of pH-induced stability changes have been made for other proteins such as barnase,[22] prolactin,[12,13] and prion protein.[14] Furthermore, histidine residues have been implicated as pH sensors in many cases.[11] To elucidate the individual contributions of the three histidine residues in CLIC1 to the observed pH-dependent conformational stability changes, we systematically mutated the three histidine residues to nonionizable alanine or phenylalanine residues. When the

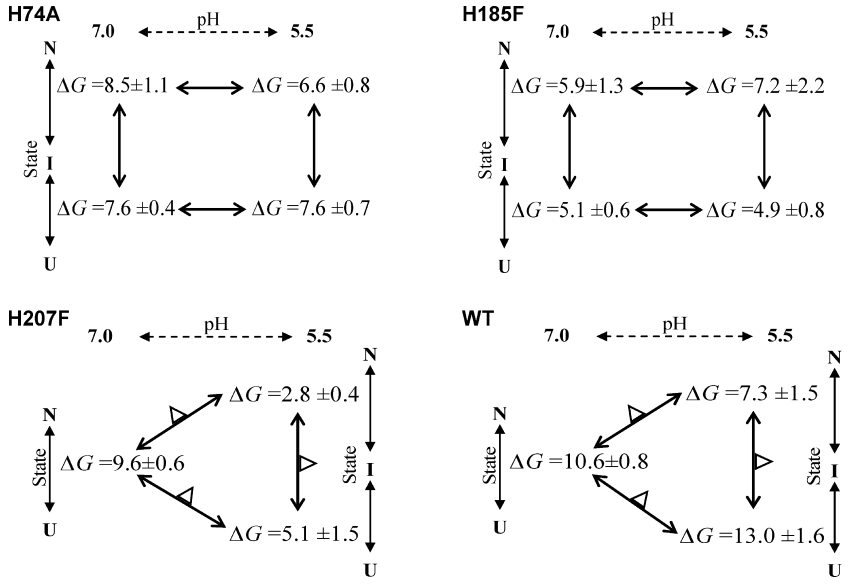

Figure 4. Schematic representation of the change in the Gibbs free energy of unfolding ΔG (kilocalories per mole) for the wild type (WT) and the three histidine mutants at pH 7.0 and 5.5. Two-state fits are indicated by a single ΔG value, while three-state fits are represented by two ΔG values: one for the N → I transition (top) and one for the I → U transition (bottom). Two-way arrows between two transition states (vertical) or across pH values (horizontal) denote the lack of significant changes in ΔG. Two-way arrows with a triangle between two transition states (vertical) or across pH values (diagonal) denote significant changes in ΔG.

dx.doi.org/10.1021/bi201541w | *Biochemistry* 2012, 51, 995–1004

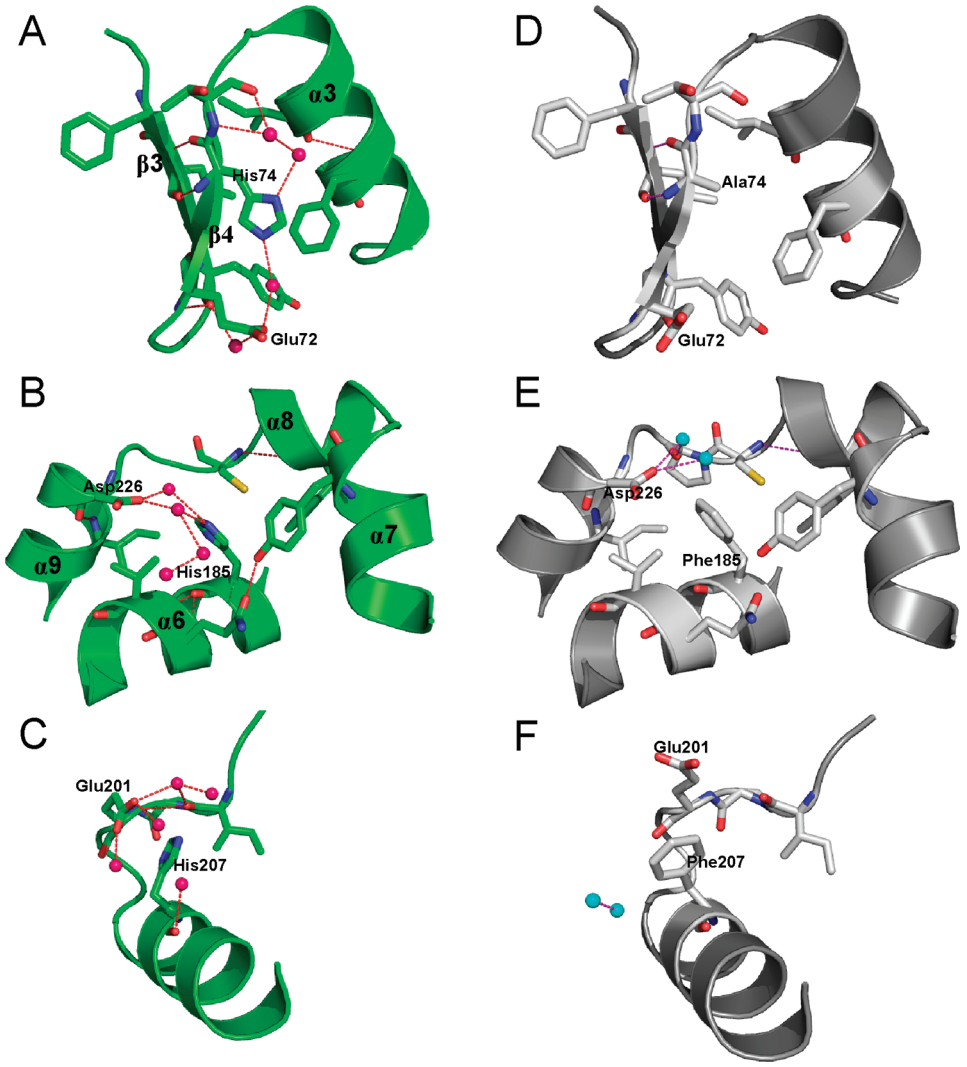

Figure 5. Change in H-bond coordination due to the replacement of the histidine residues in human CLIC1 at positions 74, 185, and 207 with alanine and phenylalanine: wild type (A–C), H74A (D), H185F (E), and H207F (F). Spheres represent water molecules forming H-bond interactions within 4 Å of the histidine residue. Dashed lines represent H-bond interactions as computed by SPDBV version 4.0.[40] The images were generated with PyMol.[41]

pH is varied from 5.5 to 7.0, it is expected that the charge on the three histidine residues will become less positive as they become deprotonated. We do note that a histidine side chain in a protein may exhibit a slightly perturbed pK_a because of the degree of exposure of the side chain to solvent and also the presence of other charged and titratable side chains within the vicinity of the histidine side chain.[14,22,23,43,44] Theoretically, however, the replacement of the histidine residues in CLIC1 with alanine or phenylalanine will eliminate any pH-dependent protonation at that position, so that the side chain of the histidine mutants will be close to neutral at pH 7.0 and 5.5. If any of the three histidine residues are involved in pH sensing, and if the protonated form at pH 5.5 is important for the pH-induced changes that we have observed with the wild type, then the mutants should behave as the wild type does at pH 7.0 when they are at pH 5.5. Furthermore, there should not be a distinct difference between the behavior of the mutant at pH 5.5 and 7.0.

The equilibrium unfolding data indicate that while the H207F mutant shows a trend similar to that of the wild type with a two-state transition at pH 7.0 and a three-state transition at pH 5.5, both the H74A and H185F mutants provide evidence of the accumulation of a stable intermediate state along their equilibrium unfolding pathways, not only at pH 5.5 but also at pH 7.0 (Figures 2 and 3). This could be due to the removal of the pH-sensitive imidazole side chain from these mutants, which causes the loss of pH sensitivity and hence the appearance of the equilibrium intermediate at both pH values. This observation may not be entirely related to histidine-mediated pH sensing, however, and we should be cautious in labeling it as such without first examining the structure of these mutants and the relevant thermodynamics. The formation of a stable intermediate at pH 7.0 in the case of these mutants could also be due to the effect of the mutation on the unfolding pathway of the protein via breakage of specific stabilizing local contacts that are not necessarily influenced by pH as has been observed with a number of other CLIC mutants that have been studied in our laboratory[45] (Legg-E'Silva, unpublished work). However, close examination of the thermodynamic parameters obtained from the unfolding of the histidine mutants provides an interesting scenario that is unlike that of any other CLIC mutant that we have studied. There is very little change in

dx.doi.org/10.1021/bi201541w | *Biochemistry* 2012, 51, 995–1004

ΔG_{NU} between the pH values ($\Delta\Delta G_{NU}$) for the histidine mutants, whereas for the wild type, the $\Delta\Delta G_{NU}$ (pH 5.5−7.0) is ∼10.0 kcal/mol (Figure 6). This suggests that the stability of the mutant proteins is no longer sensitive to a change in pH. This result corresponds to a study conducted by Keeler et al.[12] in which mutation of certain histidine residues in human prolactin produced a lower $\Delta\Delta G_{NU}$ between pH 7.8 and 5.8 compared to that of the wild type, which they attributed to a loss of pH sensitivity in the mutants.

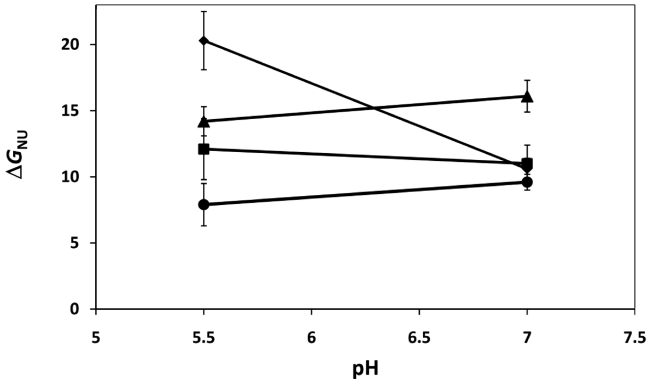

Figure 6. General trend of the relationship between ΔG_{NU} and pH. Summary of the ΔG_{NU} values of the wild type (◆), H74A (▲), H185F (■), and H207F (●) deduced from the globally fit data of the urea-induced equilibrium unfolding experiment at pH 5.5 and 7.0. These traces simply emphasize the perceptible pH-dependent trend of two data points at pH 5.5 and 7.0, and it is not a representation of a complete theoretical or empirically based pH-dependent model over the pH range indicated.

The far-UV CD studies at pH values ranging from 5.0 to 8.5 of the CLIC1 mutants suggest that the replacement of the histidine residues at the three positions did not alter the global secondary structure conformations of the mutant proteins. Thus, the observed changes in the unfolding profile of the mutants compared to that of the wild type are a result of changes in bonding interactions within the local environment of the mutants. This was confirmed by the crystal structure of the mutants, which showed that the global structure of CLIC1 was not perturbed by the mutations as evidenced by rmsd values ranging from 0.51 to 0.76 for the alignment of three mutants with the wild type. Analysis of the structural alignments (Figure 1) reveals information about the role of the three histidine residues in the structure of the protein. His74 is found in the N-domain, the more flexible of the two domains,[46] which is the one that is believed to partially unfold in response to a change in pH when at the membrane surface.[4,47] The H74A mutation breaks interactions that will cause strand β4 and possibly the β3−β4 sheet to become destabilized, resulting in the observed overall loss of stability of this mutant compared to that of the wild type (Figure 4). The mutation may also facilitate the detachment of the N-domain from the C-domain, resulting in the detection of the intermediate state, even at pH 7.0. His185 is located on helix α6 of the C-domain. It is the only one of the three CLIC1 histidine residues that is conserved across the CLIC family. Replacing this residue with a phenylalanine results in the loss of an alternating ionic bridge interaction with Asp226, which may be vital in maintaining the pH dependence of the stability[40−42] and may explain why H185F, like H74A, displays a similar unfolding profile at pH 7.0 and 5.5. His207 is located in helix α7 in the C-domain. This residue is the most solvent exposed of the three histidine residues and does not contribute to the pH-dependent trend in the stability of the protein (Figure 4). The decrease in the stability of H207F at pH 5.5 compared to that of the wild type can be explained by the introduction of the very hydrophobic phenylalanine ring into the solvent-exposed pocket that was formerly occupied by the histidine.

So, can any of the three CLIC1 histidine residues be said to be a pH sensor that causes the stability of CLIC1 to change in response to pH? Although none of the mutants display an unfolding profile at pH 5.5 that resembles that of the wild type at pH 7.0 as would be expected for the removal of a pH sensor of this nature, both H74A and H185F no longer show pH-dependent trends in their unfolding profiles, whereas H207F and the wild type do. We also notice that the total free energy change, ΔG_{NU}, of the mutants at pH 7.0 is not altered from that of the wild type, which implies a shift in the free energy change from stabilizing the native state to stabilizing the intermediate state. Therefore, examination of the stability of the intermediate state may be very telling in the analysis of what effect protonation of these histidine residues may have on CLIC1. We see that in the case of the wild type, protonation of the histidine residues increases the stability of the intermediate (ΔG_{IU} = 13 kcal/mol while ΔG_{NI} = only 7.3 kcal/mol at pH 5.5; ∼1.8 ΔG_{NI}:ΔG_{IU} ratio) (Figure 4). Removal of His207 retains a ΔG_{NI}:ΔG_{IU} ratio of approximately 1.8 (Figure 4), despite an overall loss of stability as seen in Figure 6. Upon removal of His185 or His74, however, we see both a marked decrease in the stability of the intermediate state at pH 5.5 with a ΔG_{NI}:ΔG_{IU} ratio close to 1.0 (Figure 4) and, as already mentioned, a loss of pH sensitivity of the unfolding transition so that unfolding at pH 7.0 resembles that at pH 5.5 (within error). From this information, we can conclude that perhaps the protonation state of the histidine residues does not so much affect the native state as it does the intermediate state. The intermediate state forms upon destabilization of the native state. In the case of the wild type, this is caused by a decrease in pH. The intermediate state may then become stabilized by the protonation of the histidine residues. In the case of H74A and H185F, the mutation destabilizes the native state, so the intermediate state appears even at pH 7.0. This intermediate is destabilized compared to that of the wild type because of the lack of stabilizing interactions offered by the protonated imidazole. A decrease in pH from 7.0 to 5.5 does not change the stability of the intermediate state in these two mutants and eliminates the pH-dependent changes observed in the unfolding transition. This implies that both these histidine residues may play a role in the pH-dependent changes observed in the wild type.

■ CONCLUSIONS

We conclude that both His74 and His185 are involved in triggering the pH-induced changes to the conformational stability of wild-type CLIC1 via their protonation, which stabilizes the intermediate state. Although both histidine residues are involved, their individual contributions to the process are likely to vary. This is evident in the slight variation in ΔG and unfolding behavior of each mutant. The location of His74 in the N-domain facilitates the stabilization of the membrane-competent form of the protein at low pH, while the conserved His185 on helix α6 could play a role in priming the C-domain for the new membrane-bound conformation.

■ ASSOCIATED CONTENT

Supporting Information

Detection of the presence of unfolding intermediates in CLIC1 using ANS (Figure S1) and global fitting protocol and the statistics related to the fit ("goodness of fit") (Table S1). This material is available free of charge via the Internet at http://pubs.acs.org.

■ AUTHOR INFORMATION

Corresponding Author

*E-mail: heinrich.dirr@wits.ac.za. Telephone: +27 11 7176352. Fax: +27 11 717 6351.

Funding

This work was supported by the University of the Witwatersrand, the South African National Research Foundation (Grants 60810, 65510, and 68898 to H.W.D.), and the South African Research Chairs Initiative of the Department of Science and Technology and National Research Foundation (Grant 64788 to H.W.D.). This work was also supported by the Carnegie Foundation.

■ ABBREVIATIONS

CLIC, chloride intracellular channel; CD, circular dichroism; GST, glutathione *S*-transferase; ANS, 8-anilino-1-naphthalenesulfonate; far-UV, far-ultraviolet; PDB, Protein Data Bank.

■ REFERENCES

(1) al-Awqati, Q. (1995) Chloride channels of intracellular organelles. *Curr. Opin. Cell Biol. 7*, 504−508.

(2) Littler, D. R., Harrop, S. J., Goodchild, S. C., Phang, J. M., Mynott, A. V., Jiang, L., Valenzuela, S. M., Mazzanti, M., Brown, L. J., Breit, S. N., and Curmi, P. M. (2010) The enigma of the CLIC proteins: Ion channels, redox proteins, enzymes, scaffolding proteins? *FEBS Lett. 584*, 2093−2101.

(3) He, G., Ma, Y., Chou, S. Y., Li, H., Yang, C., Chuang, J. Z., Sung, C. H., and Ding, A. (2011) Role of CLIC4 in the host innate responses to bacterial lipopolysaccharide. *Eur. J. Immunol. 41*, 1221−1230.

(4) Goodchild, S. C., Howell, M. W., Littler, D. R., Mandyam, R. A., Sale, K. L., Mazzanti, M., Breit, S. N., Curmi, P. M., and Brown, L. J. (2010) Metamorphic response of the CLIC1 chloride intracellular ion channel protein upon membrane interaction. *Biochemistry 49*, 5278−5289.

(5) Fanucchi, S., Adamson, R. J., and Dirr, H. W. (2008) Formation of an unfolding intermediate state of soluble chloride intracellular channel protein CLIC1 at acidic pH. *Biochemistry 47*, 11674−11681.

(6) Cromer, B. A., Morton, C. J., Board, P. G., and Parker, M. W. (2002) From glutathione transferase to pore in a CLIC. *Eur. Biophys. J. 31*, 356−364.

(7) Harrop, S. J., DeMaere, M. Z., Fairlie, W. D., Reztsova, T., Valenzuela, S. M., Mazzanti, M., Tonini, R., Qiu, M. R., Jankova, L., Warton, K., Bauskin, A. R., Wu, W. M., Pankhurst, S., Campbell, T. J., Breit, S. N., and Curmi, P. M. (2001) Crystal structure of a soluble form of the intracellular chloride ion channel CLIC1 (NCC27) at 1.4-Å resolution. *J. Biol. Chem. 276*, 44993−45000.

(8) Tulk, B. M., Schlesinger, P. H., Kapadia, S. A., and Edwards, J. C. (2000) CLIC-1 functions as a chloride channel when expressed and purified from bacteria. *J. Biol. Chem. 275*, 26986−26993.

(9) Mynott, A. V., Harrop, S. J., Brown, L. J., Breit, S. N., Kobe, B., and Curmi, P. M. (2011) Crystal structure of importin-α bound to a peptide bearing the nuclear localisation signal from chloride intracellular channel protein 4. *FEBS J. 278*, 1662−1675.

(10) Poirot, O., Suhre, K., Abergel, C., O'Toole, E., and Notredame, C. (2004) 3DCoffee@igs: A web server for combining sequences and structures into a multiple sequence alignment. *Nucleic Acids Res. 32*, W37−W40.

(11) Srivastava, J., Barber, D. L., and Jacobson, M. P. (2007) Intracellular pH sensors: Design principles and functional significance. *Physiology 22*, 30−39.

(12) Keeler, C., Tettamanzi, M. C., Meshack, S., and Hodsdon, M. E. (2009) Contribution of individual histidines to the global stability of human prolactin. *Protein Sci. 18*, 909−920.

(13) Tettamanzi, M. C., Keeler, C., Meshack, S., and Hodsdon, M. E. (2008) Analysis of site-specific histidine protonation in human prolactin. *Biochemistry 47*, 8638−8647.

(14) Langella, E., Improta, R., and Barone, V. (2004) Checking the pH-induced conformational transition of prion protein by molecular dynamics simulations: Effect of protonation of histidine residues. *Biophys. J. 87*, 3623−3632.

(15) Gerchman, Y., Olami, Y., Rimon, A., Taglicht, D., Schuldiner, S., and Padan, E. (1993) Histidine-226 is part of the pH sensor of NhaA, a Na^+/H^+ antiporter in *Escherichia coli*. *Proc. Natl. Acad. Sci. U.S.A. 90*, 1212−1216.

(16) Sobko, A. A., Rokitskaya, T. I., and Kotova, E. A. (2009) Histidine 440 controls the opening of colicin E1 channels in a lipid-dependent manner. *Biochim. Biophys. Acta 1788*, 1962−1966.

(17) Krantz, B. A., Trivedi, A. D., Cunningham, K., Christensen, K. A., and Collier, R. J. (2004) Acid-induced unfolding of the amino-terminal domains of the lethal and edema factors of anthrax toxin. *J. Mol. Biol. 344*, 739−756.

(18) Rodnin, M. V., Kyrychenko, A., Kienker, P., Sharma, O., Posokhov, Y. O., Collier, R. J., Finkelstein, A., and Ladokhin, A. S. (2010) Conformational switching of the diphtheria toxin T domain. *J. Mol. Biol. 402*, 1−7.

(19) Nelson, S., Poddar, S., Lin, T. Y., and Pierson, T. C. (2009) Protonation of individual histidine residues is not required for the pH-dependent entry of West Nile Virus: Evaluation of the "histidine switch" hypothesis. *J. Virol. 83*, 12631−12635.

(20) Dang, L. T., Purvis, A. R., Huang, R. H., Westfield, L. A., and Sadler, J. E. (2011) Phylogenetic and functional analysis of histidine residues essential for pH-dependent multimerization of von Willebrand factor. *J. Biol. Chem. 286*, 25763−25769.

(21) Tulk, B. M., Kapadia, S., and Edwards, J. C. (2002) CLIC1 inserts from the aqueous phase into phospholipid membranes, where it functions as an anion channel. *Am. J. Physiol. 282*, C1103−C1112.

(22) Warton, K., Tonini, R., Fairlie, W. D., Matthews, J. M., Valenzuela, S. M., Qiu, M. R., Wu, W. M., Pankhurst, S., Bauskin, A. R., Harrop, S. J., Campbell, T. J., Curmi, P. M., Breit, S. N., and Mazzanti, M. (2002) Recombinant CLIC1 (NCC27) assembles in lipid bilayers via a pH-dependent two-state process to form chloride ion channels with identical characteristics to those observed in Chinese hamster ovary cells expressing CLIC1. *J. Biol. Chem. 277*, 26003−26011.

(23) Shimidzu, M., Shindo, H., Matsumoto, U., Mita, K., and Zama, M. (1985) Involvement of the histidine residues in the pH-induced conformational change of histone H5. *Arch. Biochem. Biophys. 241*, 692−695.

(24) Loewenthal, R., Sancho, J., and Fersht, A. R. (1992) Histidine-aromatic interactions in barnase: Elevation of histidine pKa and contribution to protein stability. *J. Mol. Biol. 224*, 759−770.

(25) Sancho, J., Serrano, L., and Fersht, A. R. (1992) Histidine residues at the N- and C-termini of α-helices: Perturbed pKas and protein stability. *Biochemistry 31*, 2253−2258.

(26) Horng, J. C., Cho, J. H., and Raleigh, D. P. (2005) Analysis of the pH-dependent folding and stability of histidine point mutants allows characterization of the denatured state and transition state for protein folding. *J. Mol. Biol. 345*, 163−173.

(27) Grey, M., Tang, Y., Alexov, E., McKnight, C., Raleigh, D., and Palmer, A. G. III (2006) Characterizing a Partially Folded Intermediate of the Villin Headpiece Domain Under Non-denaturing Conditions: Contribution of His41 to the pH-dependent stability of the N-terminal Subdomain. *J. Mol. Biol. 355*, 1078−1094.

(28) Laemmli, U. K. (1970) Cleavage of structural proteins during the assembly of the head of bacteriophage T4. *Nature 227*, 680−685.

(29) Beechem, J. M. (1992) Global analysis of biochemical and biophysical data. *Methods Enzymol. 210*, 37−54.

(30) Bilsel, O., Zitzewitz, J. A., Bowers, K. E., and Matthews, C. R. (1999) Folding mechanism of the α-subunit of tryptophan synthase, an α/β barrel protein: Global analysis highlights the interconversion of multiple native, intermediate, and unfolded forms through parallel channels. *Biochemistry 38*, 1018−1029.
(31) Pace, C. N. (1986) Determination and analysis of urea and guanidine hydrochloride denaturation curves. *Methods Enzymol. 131*, 266−280.
(32) McCoy, A. J. (2007) Solving structures of protein complexes by molecular replacement with Phaser. *Acta Crystallogr. 63*, 32−41.
(33) McCoy, A. J., Grosse-Kunstleve, R. W., Adams, P. D., Winn, M. D., Storoni, L. C., and Read, R. J. (2007) Phaser crystallographic software. *J. Appl. Crystallogr. 40*, 658−674.
(34) Collaborative Computational Project Number 4 (1994) The CCP4 suite: Programs for protein crystallography. *Acta Crystallogr. 50*, 760−763.
(35) Joosten, R. P., Womack, T., Vriend, G., and Bricogne, G. (2009) Re-refinement from deposited X-ray data can deliver improved models for most PDB entries. *Acta Crystallogr. 65*, 176−185.
(36) Murshudov, G. N., Vagin, A. A., and Dodson, E. J. (1997) Refinement of macromolecular structures by the maximum-likelihood method. *Acta Crystallogr. 53*, 240−255.
(37) Emsley, P., and Cowtan, K. (2004) Coot: Model-building tools for molecular graphics. *Acta Crystallogr. 60*, 2126−2132.
(38) Laskowski, R. A., Rullmannn, J. A., MacArthur, M. W., Kaptein, R., and Thornton, J. M. (1996) AQUA and PROCHECK-NMR: Programs for checking the quality of protein structures solved by NMR. *J. Biomol. NMR 8*, 477−486.
(39) Chen, V. B., Arendall, W. B. III, Headd, J. J., Keedy, D. A., Immormino, R. M., Kapral, G. J., Murray, L. W., Richardson, J. S., and Richardson, D. C. (2010) MolProbity: All-atom structure validation for macromolecular crystallography. *Acta Crystallogr. 66*, 12−21.
(40) Guex, N., and Peitsch, M. C. (1997) SWISS-MODEL and the Swiss-PdbViewer: An environment for comparative protein modeling. *Electrophoresis 18*, 2714−2723.
(41) DeLano, W. L. (2002) *The PyMOL Molecular Graphics System*, DeLano Scientific, San Carlos, CA.
(42) Winayanuwattikun, P., and Ketterman, A. J. (2007) Glutamate-64, a newly identified residue of the functionally conserved electron-sharing network contributes to catalysis and structural integrity of glutathione transferases. *Biochem. J. 402*, 339−348.
(43) Wongsantichon, J., and Ketterman, A. J. (2005) Alternative splicing of glutathione S-transferases. *Methods Enzymol. 401*, 100−116.
(44) Winayanuwattikun, P., and Ketterman, A. J. (2005) An electron-sharing network involved in the catalytic mechanism is functionally conserved in different glutathione transferase classes. *J. Biol. Chem. 280*, 31776−31782.
(45) Parbhoo, N., Stoychev, S. H., Fanucchi, S., Achilonu, I., Adamson, R. J., Fernandes, M., Gildenhuys, S., and Dirr, H. W. (2011) A Conserved Interdomain Interaction Is a Determinant of Folding Cooperativity in the GST Fold. *Biochemistry 50*, 7067−7075.
(46) Stoychev, S. H., Nathaniel, C., Fanucchi, S., Brock, M., Li, S., Asmus, K., Woods, V. L. Jr., and Dirr, H. W. (2009) Structural dynamics of soluble chloride intracellular channel protein CLIC1 examined by amide hydrogen-deuterium exchange mass spectrometry. *Biochemistry 48*, 8413−8421.
(47) Tonini, R., Ferroni, A., Valenzuela, S. M., Warton, K., Campbell, T. J., Breit, S. N., and Mazzanti, M. (2000) Functional characterization of the NCC27 nuclear protein in stable transfected CHO-K1 cells. *FASEB J. 14*, 1171−1178.